Acta Mechanica Slovaca **28 (2): 6 -21 ,** Jun **2024**
https://doi.org/10.21496/ams.2024.008

Acta Mechanica Slovaca
ISSN 1335-2393
www.actamechanica.sk

A Numerical Study of the Innovative Design of Kinetic Static Mixer on Mixing Efficiency and Heat Transfer Improvement

Ourdia Benabdellaziz [1*], Youcef Kamla [2], Ahmed Mouissi [3], Abdelkader Karas [4], Zied Driss [5]

1 Laboratory of Rheology and Mechanics (LRM), Mechanical Engineering department, Faculty of Technology, Hassiba BenBouali University of Chlef, Algeria
2 Laboratory for Theoretical Physics and Material Physics (LPTPM), Faculty of Technology, Hassiba BenBouali University of Chlef, Algeria
3 Laboratory of Industrial fluids, Measurement and Application, Faculty of Science and Technology Khemis Miliana university, Algeria
4 Mechanical Engineering department, Faculty of Technology, University Ibn Khaldoun, Tiaret, Algérie
5 Laboratory of Electromechanical Systems (LASEM), National School of Engineers of Sfax (ENIS), University of Sfax, Tunisia

Abstract: This paper investigates the influence of rheological and geometrical properties on flow structures generated within a KENIC static mixer. The primary objectives are to examine the impact of these factors on fluid flow characteristics, particularly low-pressure conditions and mixing efficiency. To exanimate the performances of the different shapes, several parameters have been considered which consist on mixing index, thermal mixing index, hydrodynamic behavior and the probability density function. The investigation extends to encompass both Newtonian and non-Newtonian fluids, emphasizing Reynolds numbers ranging from 10 to 80. Comparative analyses are conducted against a conventional static mixer configuration. However, this investigation has been done with a numerical simulation using Ansys 20. Through comprehensive numerical simulations, the study highlights the significance of rheological and geometrical factors in shaping flow behaviors. The findings underscore the superior performance of the KENIC static mixer's designated configuration, denoted as KMSFH, when contrasted with alternative scenarios. The improved performance is observed across various flow conditions, showcasing enhanced mixing efficiency and lower pressure losses. Overall, this study found that the KMSFH showed a better performance with 99% than the other suggested mixers.

Keywords: Mixing; Kenic; Drop pressur; Nusselt

1. Introduction

Mixing processes are widely encountered in many industrial processes. In fact, the homogenization and transformation processes, physical or chemical, of matter or energy transfer are the basis of many industrial sectors such as ago-food, petrochemicals, pharmaceuticals, cosmetics, stationery, etc. The mixing or extraction processes depend mainly on their mass. power transmission capabilities, efficiency, and energy consumption. Research and development of mixing technology is an active area of research in physics and chemical engineering due to its increasing importance in many sectors of industry. Mixing can be achieved by intermittent and semi-intermittent operation using conventional mechanical agitators, or by continuous processes Mahmoodi et al. [1–3]. In the latter case, stationary mixers are usually used. For the mixture to be homogeneous, the different components must be in motion. This mobility during the mixing process is mainly due to the convection, shear and diffusion mechanisms but also to the technological capabilities of the mixing devices. When two or more liquids are mixed, the first phenomenon is the mixing of the existing liquids.

*** Corresponding author:** Ourdia Benabdellaziz ***E-mail address:*** *o.benabdellaziz95@univ-chlef.dz*

Mixing is an essential component of almost all industrial processes, from simple mixing of liquids of different compositions or temperatures to complex chemical reactions whose production and reaction selectivity strongly depends on mixing performance. Selectivity is the key aspect of any reactive process as it is known that the profitability of the process can vary with changes as low as 1% of its selectivity Meng et al. [4–6]. Before continuing, it is important to clarify a number of concepts used in this work. Under this broad mix, different processes and several general input mechanisms are involved. According to Abushaikha et al [7-8], a static mixer consists of an ordinary tube in which static mixing elements have been placed. The static mixers market offers a wide variety of designs. Since these designs have very different geometric characteristics, it makes it possible to initially classify them according to their morphology. Moreover, each mixer morphology generates a flow with its own characteristics. Thus, it is possible to classify the different mixers according to the type of flow they generate and, accordingly, according to the type of mixing process for which they can be used.

Belhout. et al., [9–10] investigated the effect of several geometric parameters of a KENIC-type static mixer on heat transfer. HOOBS et al. [11], Ghanem et al. [12] and Rauline et al. [13] Several simulations to study the effect of the laminar flow system and turbulence on the performance of the static mixer, the geometry of the Sulzer SMX static mixer was modified and studied numerically by Sumana et al., [14], Ameur et al [15] and Talhaoui et al [16] Haddadi et al. [17-18] investigated the mechanism, applications and characterization methods of the static mixer. The effect of Reynolds number, fluid viscosity, P* ratio, and then the number of mixing elements on flow patterns and pressure drop were studied Ghanem et al. [19-20] Computer simulation of Kenics, in Liner, LPD, Cleveland, SMX and ISG static mixers.

This numerical study aims to improve our comprehension of fluid mixing in various static mixers, each of which has a unique shape. The objective of the investigation is to examine how mixing parts affect mixer performance, as well as how changes in those components' forms affect that performance. However, this study examinate four different shapes and compared them with standard.

2. Geometry simulated

In this study, the three-dimensional geometry of the static mixer was studied using ansys fluent 20.0 software. the simulation was performed to study the effect of heat transfer parameters in a static mixer with four different modified cases. a cylindrical pipe and a kenic helical static mixer were designed as shown in figure 1. The dimensions of the cylindrical pipe are length L, diameter D and thickness W. They are shown in Table 1. The MS is composed of six main fixed elements. Helical shape (L/6).

The instances that have been modified from those in the static mixers are depicted in Figures 2 (a) through (e). There are three third cases, which are depicted in the illustrations below: Standard Case, a static mixer, First Case with one Hole, Second Case with two Hole, Third Case with three Hole, and Fourth Case with four Hole. The holes in the redesigned case rotate between 0° and 90° with identical static mixer rotations.

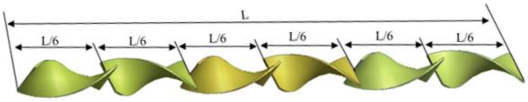

Figure 1: Case Standard

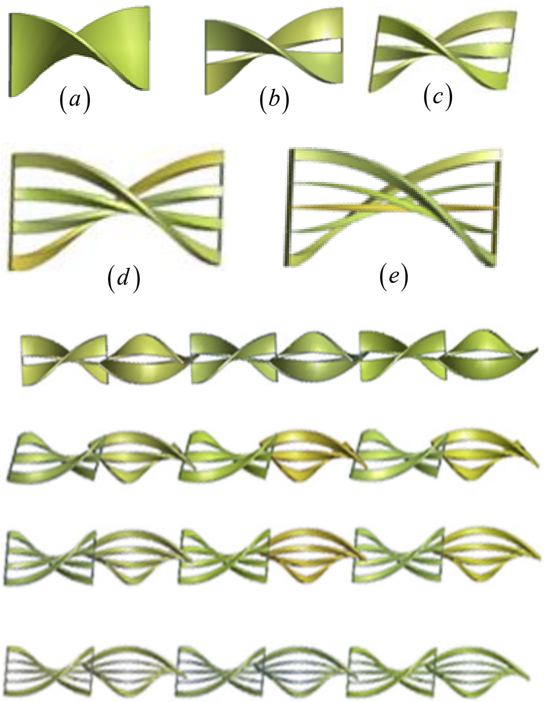

Figure 2: Different cases studied, (a) Case Standard, (b) Case KMSOH, (c) Case KMSTH and (d) Case KMSTHH, (e) Case KMSFH.

Table 1: Dimensions of the Kenics static mixer

Length , *L (m)*	Diameter, *D (m)*	Thickness, *W (m)*	Angle α
0.870	0.050	0.0032	90°

3. Physical properties of fluids

In this study, the non-Newtonian power-law fluid chosen for this study was an aqueous solution of carboxymethylcellulose (CMC) produced by Hercules Inc. (grade 7H4C), prepared by mixing CMC powder in water. This solution had concentrations of 0.1, 0.25 and 0.7%. These concentrations determine the rheological nature of the solution. Thanks to these concentrations, we were able to determine the material consistency (m) and structural index (n) of the CMC solution, as shown in the following table

The density of CMC solutions according to (2006), is 1000 kg/m^3.

Table 2: Physical properties of fluids: Fellouah et al. (2010); Pinho et al. (1990).

CMC (%)	*n(–)*	*m (pa.sn)*
0.7	0.49	2.75
0.25	0.75	0.097
0.1	0.93	0.0066

The Reynolds number generalizes Reg established by Delaplace and Leelite, for the power law model across rectangular sections of different aspect ratios is d defined as:

$$\mathrm{Re}_g = \frac{\rho V^{2-n} D_h^n}{\frac{k}{8}\left(\frac{6n+2}{2}\right)^n} \quad (1)$$

4. Mathematical and numerical modeling of the flow

In this simulation, the stationary storage equations of the incompressible fluid are numerically solved using the ANSYS Fluent 20.0 numerical fluid dynamics (CFD) code. The specific equations are as follows:

» *Conservation of mass:*

$$\nabla \vec{V} = 0 \quad (2)$$

» *Momentum conservation equation:*

$$\left(\nabla \vec{V}\right)\vec{V} = -\frac{1}{\rho}\nabla P + \nabla \overline{\overline{\tau}} \quad (3)$$

» *Conservation of energy equation :*

$$\rho c V \nabla T = \lambda \nabla^2 T \quad (4)$$

Or V , ρ , P et τ represent respectively the fluid velocity, fluid density, fluid pressure, and shear stress tensor. The shear stress tensor is written as:

$$\overline{\overline{\tau}} = \mu_a \overline{\overline{\gamma}} \quad (5)$$

Or γ is the strain rate tensor

$$\overline{\overline{\gamma}} = \nabla V + \nabla V^T \quad (6)$$

The exponent indicates the transpose operator. The deformation rate is defined as

$$\gamma = \sqrt{1/2\left(\overline{\overline{\gamma}} : \overline{\gamma}\right)} \quad (7)$$

5. Mixing model

The species transport model is most commonly used for mixing miscible fluids where the mass diffusion coefficient is considered. (SIMPLEC) the algorithm used to solve the pressure-velocity coupled equations is (SIMPLEC). A second-order wind scheme used for the discretization of momentum equations as well as the species transport equation. The convergence criterion in all simulations is taken lower than 10^{-6}.

To solve the conservation equations of fluid species, ANSYS Fluent predicts the local mass fraction Ci of each species by solving the convection-diffusion equation for the in the species. This conservation equation takes the following general form:

$$\nabla\left(\rho V C_i\right) = -\nabla j_i \quad (8)$$

Or Ji represents the term mass diffusion flux of fluid species. This flux is the result of two mechanisms: the first comes from the presence of concentration gradients, the second is the IE at pressure gradients that can cause a diffusive motion in the mixture. By default, ANSYS Fluent uses the diluted approximation (also called Fick's law) to model mass scattering due to concentration gradients, the scatter flow is written as follows:

$$J_i = D_i \nabla(\rho C_i) \quad (9)$$

D_i: Is the mass diffusion coefficient of the "i" species in the mixture. The species transport equation for a fluid of constant density and viscosity becomes

$$(V\nabla)C_i = D_i \nabla^2 C_i \quad (10)$$

The diffusion coefficient equal to 1, 10 and 11m²/s (Das, et al. 2009). Also, by this hypothesis, the mixture is governed mainly by the chaotic advection which is the most dominant mechanism. As boundary conditions, a non-slip speed condition applied to the wall surfaces, a constant uniform velocity imposed on the inlets and a pressure outlet condition is imposed on the outlet section. In addition, the mass fraction at inlet (1) is equal to 1 and at inlet (2) is equal to 0.

5.1. Mixing performance for the proposed mixers (MI)

To ensure the effectiveness of the different mixers studied, it is necessary to quantify the quality of the mixture. Therefore, we need to calculate the mixing index (MI) in each slice plane perpendicular to the flow direction.

$$MI = 1 - \frac{\sigma}{\sigma_\circ} \quad (11)$$

Or σ represents the standard deviation of the mass fraction to the cross-section d defined as:

$$\sigma^2 = \frac{1}{N}\sum_{i=1}^{N}\left(c_i - \bar{c}\right)^2 \quad (12)$$

Or N is the number of cells within the cross-section plane, (c) is the average mass fraction.

$$\sigma_\circ^2 = \bar{c}\left(1 - \bar{c}\right) \quad (13)$$

The highest standard deviation, etc. The range of mixing degrees (MI) is 0 to 1. When both fluids are fully combined, the mixing degree is 1, meaning 1. The two-phase fluids are separated when the mixing degree is zero. This implies that the mixing performance improves as the mixing degree value increases.

6. Numerical Validation

In order to validate the simulations, a comparison was conducted with the findings of Mohammedi et al. (2000). This comparison revealed promising results, demonstrating deviations of less than 33%. Furthermore, Figure 3 illustrates the evolution of the mixing index across Reynolds numbers for a Newtonian fluid.

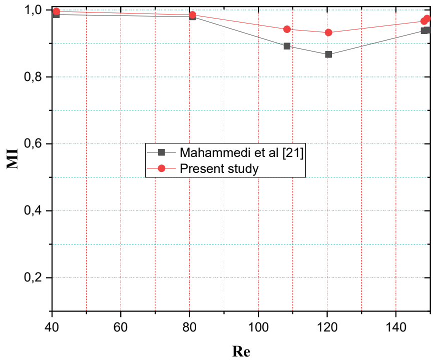

Figure 3: Evolution of mixing index of Reynolds numbers for a Newtonian fluid compared with Mahammedi et al [21].

7. Evolution of the mixing index in mixers

The chaotic mixture was examined in a mixer to determine the effects of the Reynolds number and the behavior index on the mechanism. It displays the refractive characteristics of the bulk in the planes of each mixer using various behavioral indicators and Reynolds numbers. As the flow continues, the fluid gradually separates into numerous thinner layers, as seen in Figures 1, 2, 3, and 4. The mix has been greatly enhanced. In each mixer, a homogenous mixture is produced at the output for all mixing index values and regardless of the Reynolds number value, which represents the mixer's efficacy Figures.1, 2 and 3 depict the development of the mixing index along mixers, in particular in planes 1 and 6, for various values of the index behavior and the Reynolds number, where it can reach a maximum value of 0.99 %.The mixing index at the output of the fine mixer KMSFH is shown to vary based on the Reynolds number and various behavior index values in Figure 2, it can be observed that the mixing index undergoes a variation of nearly 1, reaching its maximum value of 0.99.

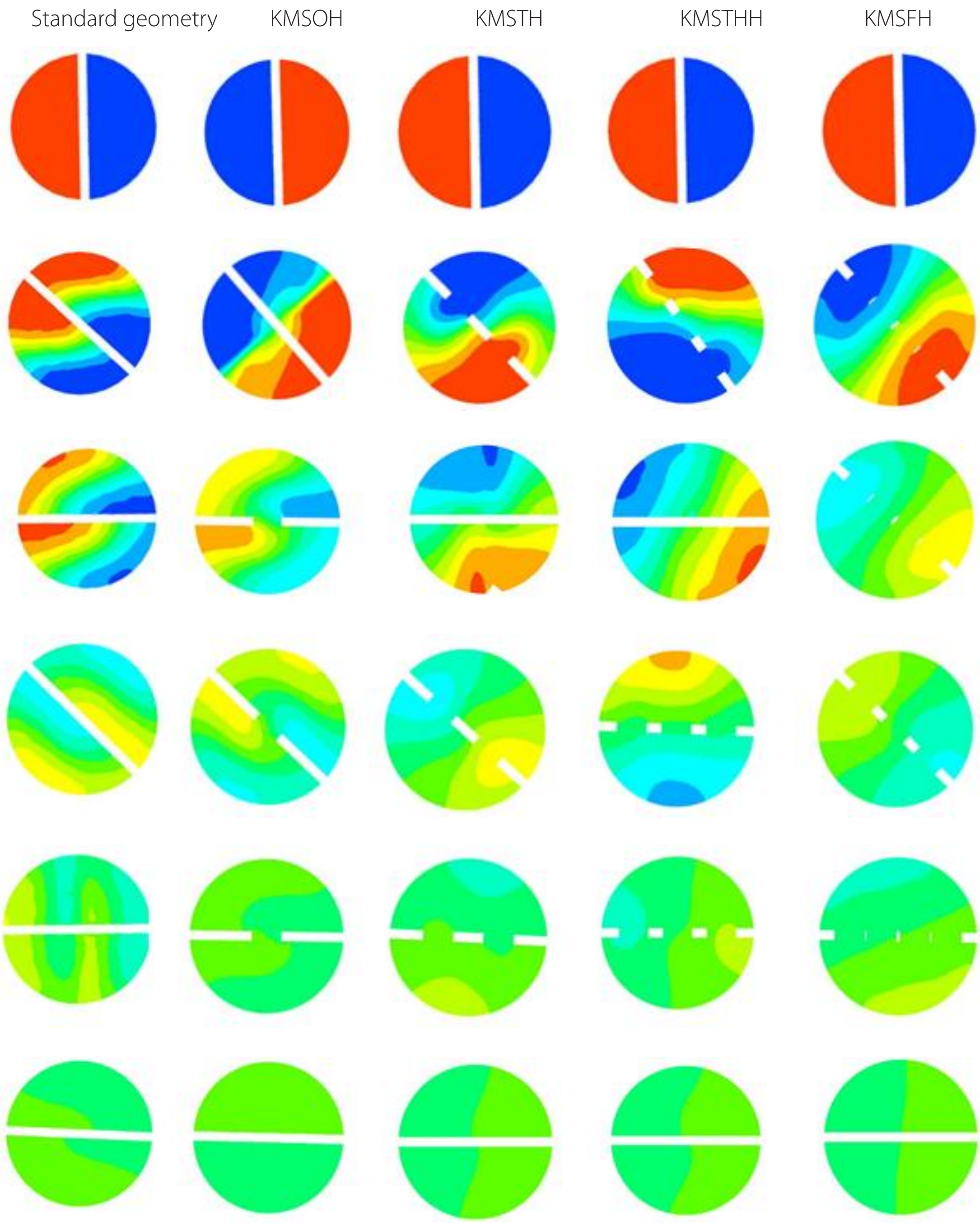

Figure 4: Mass fraction distribution in different planes at different geometries for Re= 50, n =0.75.

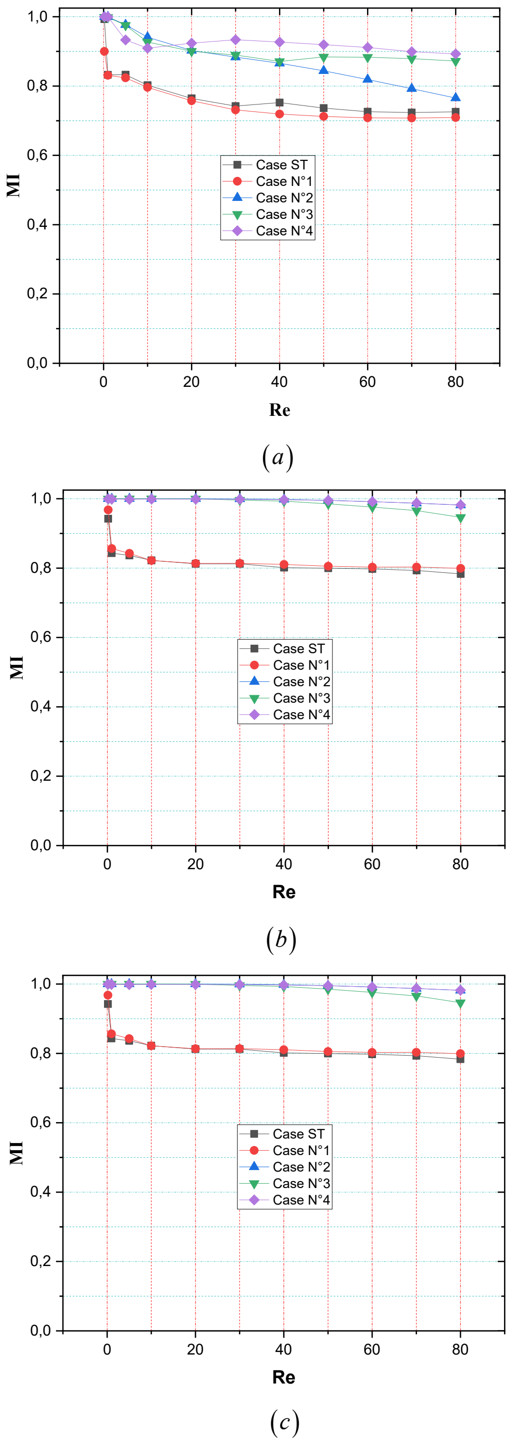

Figure 5: Variation of the mixing index at the output with Reynolds numbers for all geometries (a) n = 0.49, (b) n = 0.75, (c) n = 0.93

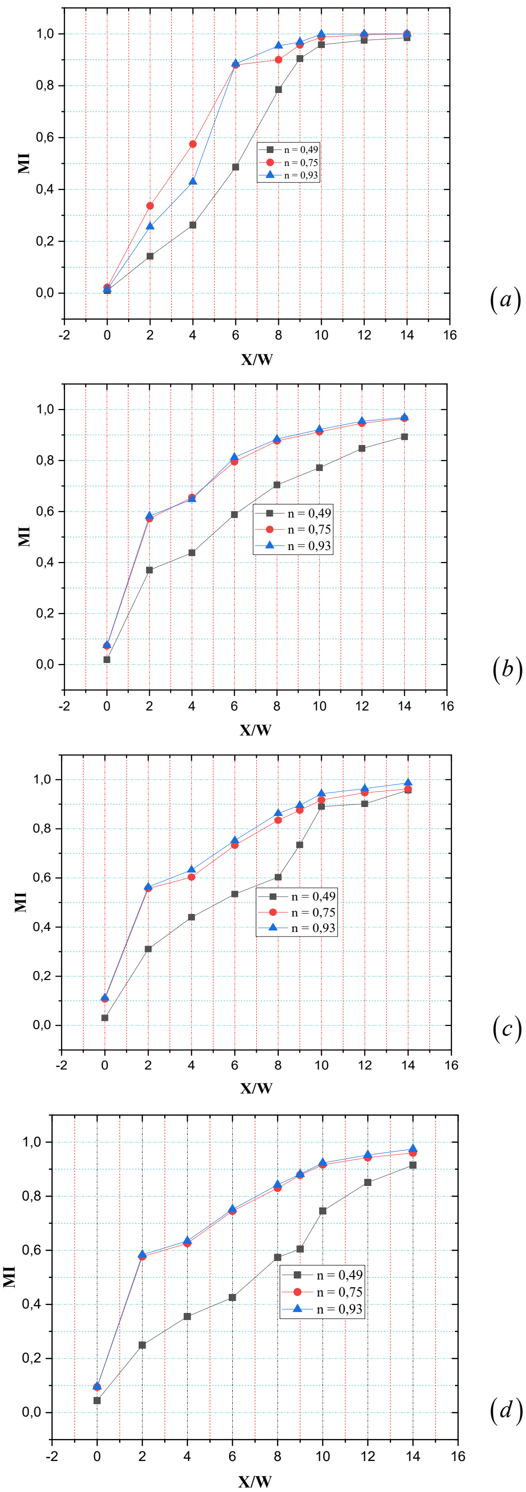

Figure 6: Evolution of mixing degree at cough outlet geometries (a: KMSOH, b: KMSTH, c: KMSTHH, d: KMSFH) as a function of distance traveled by different behavioral indices (Re=80).

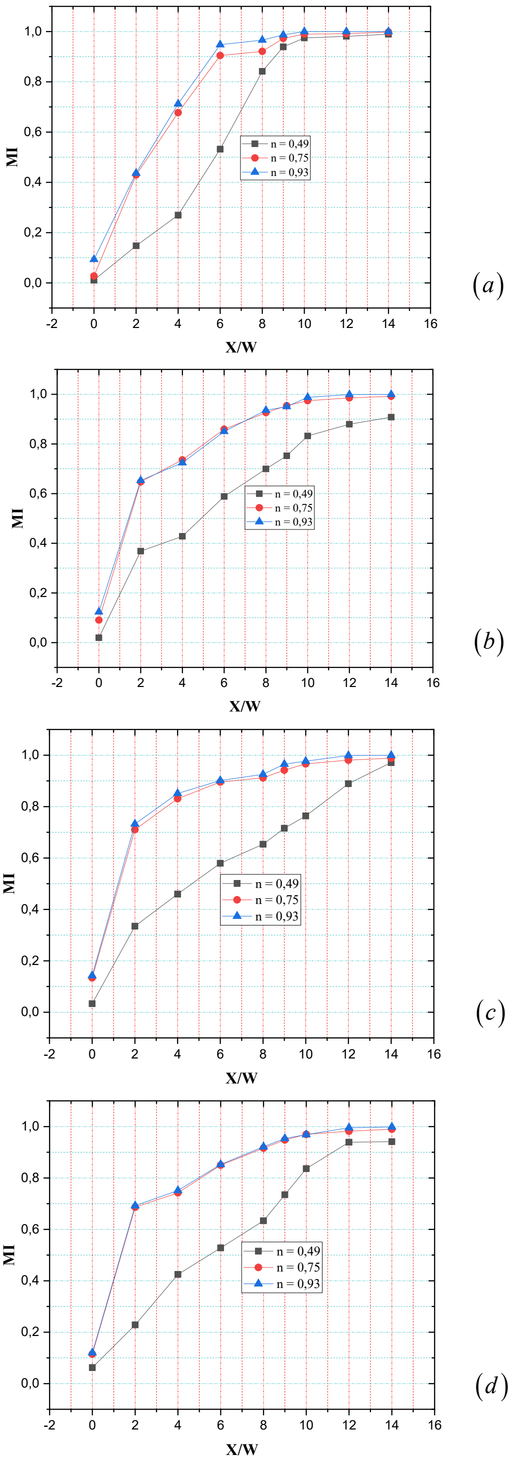

Figure 7: Evolution of mixing degree at cough outlet geometries (a: KMSOH, b: KMSTH, c: KMSTHH, d: KMSFH) as a function of distance traveled, different behavioral indices (Re=50).

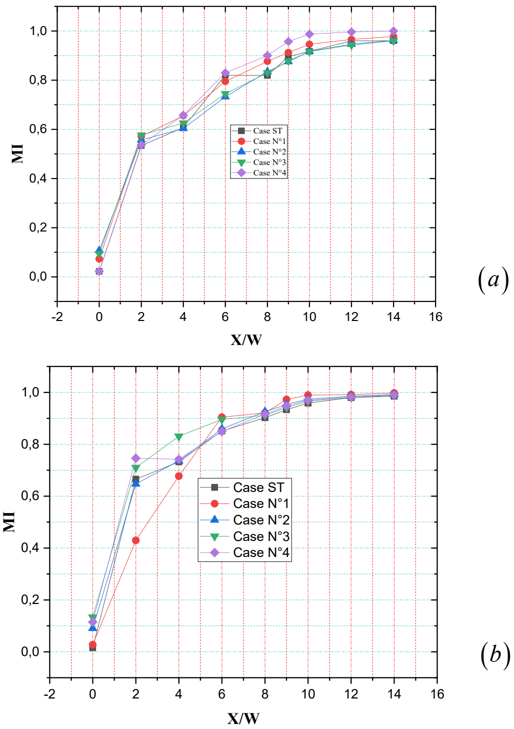

Figure 8: Evolution of the degree of thermal mixing at the cough exit plane different geometries depending on the distance traveled different behavioral indices (n = 0.75; (a) Re =80, (b) Re =50).

8. Comparison of hydrodynamic behavior and flow structure between the mixer

It is important to depict the flow field in a cross-section to better describe the structure of secondary flows; for this reason, the profiles of velocity rates in various geometries are provided in the pictures. For a reg Generalized Reynolds Number of 10; 80 and a behavior index ranging from 0.49; 0.75 to 0.93. The radial velocity rate is superior to the tangential velocity rate when compared in the center of all the geometries taken into consideration.

Due to chaotic advection, fluid particles in the crossing regions of the KMSFH geometry exhibit a stronger exchange dynamic (compression and stretching) than those in other regions of the geometry.

As seen in the following figures, the KMSFH geometry also produces a symmetry of the radial and tangential velocity rate profiles, which can be used as an additional advantage to enhance the mixture's hydrodynamic and thermal performance in comparison to other configurations.

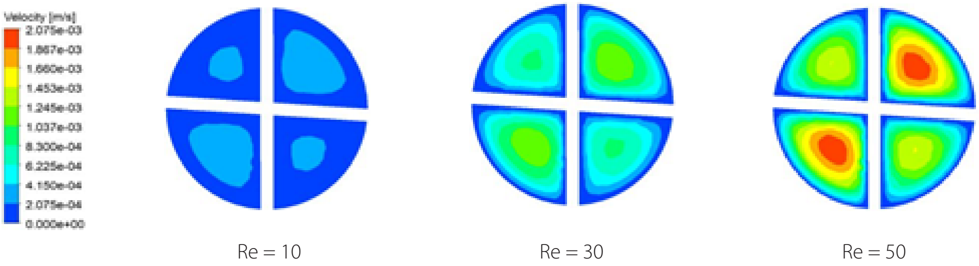

Figure 9: Velocity field for original case at Z=0.23m

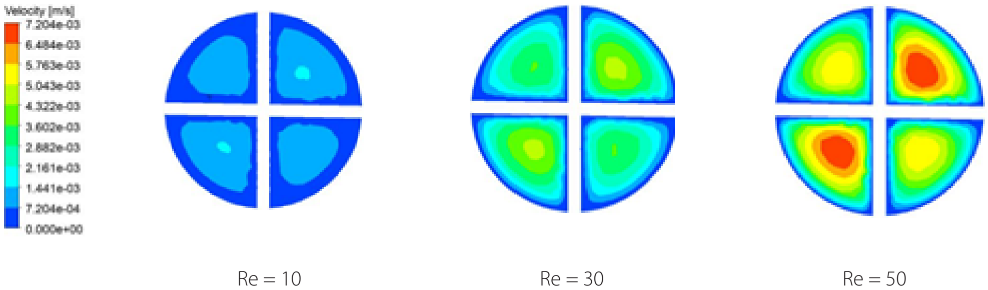

Figure 10: Velocity field for case N°1 at Z=0.23m

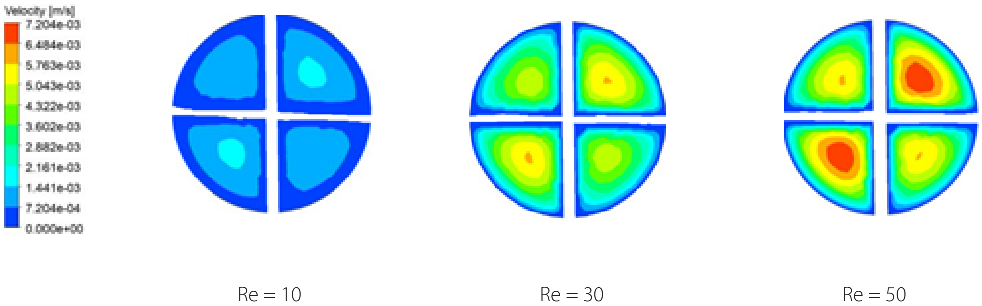

Figure11: Velocity field for case N°2 at Z=0.23

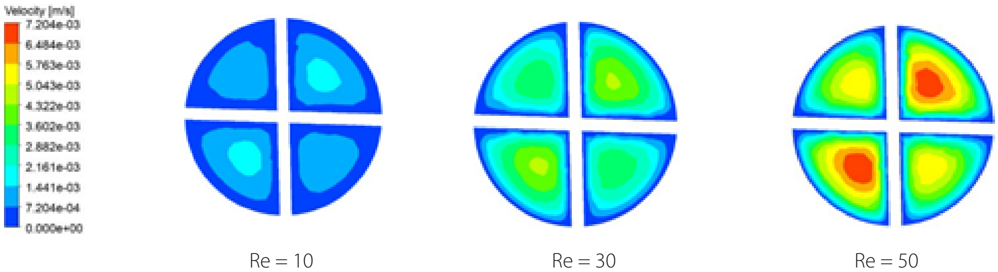

Figure 12: Velocity field for case N°3 at Z=0.23m

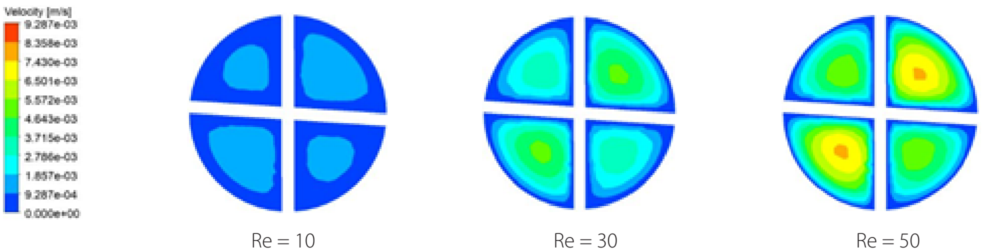

Figure 13: Velocity field for case N°4 at Z=0.23

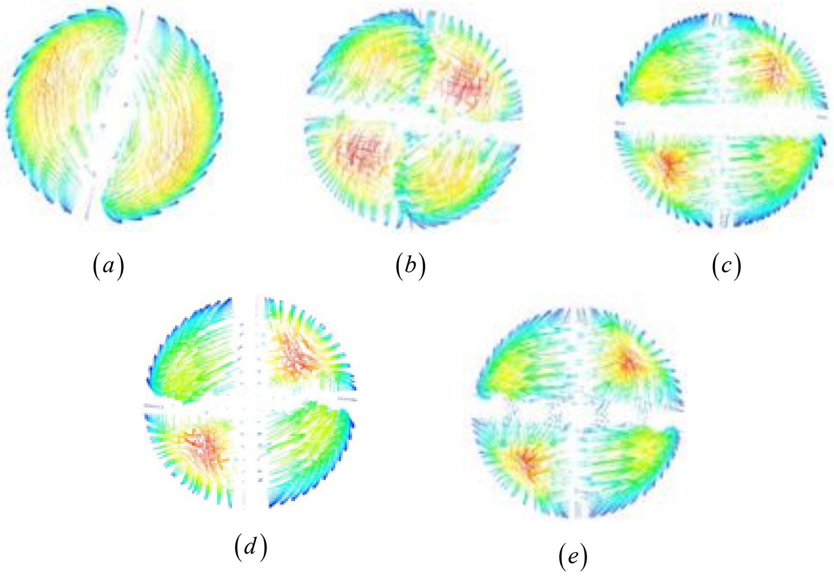

Figure 14: Vector Velocity for different geometry at Z=0.23m

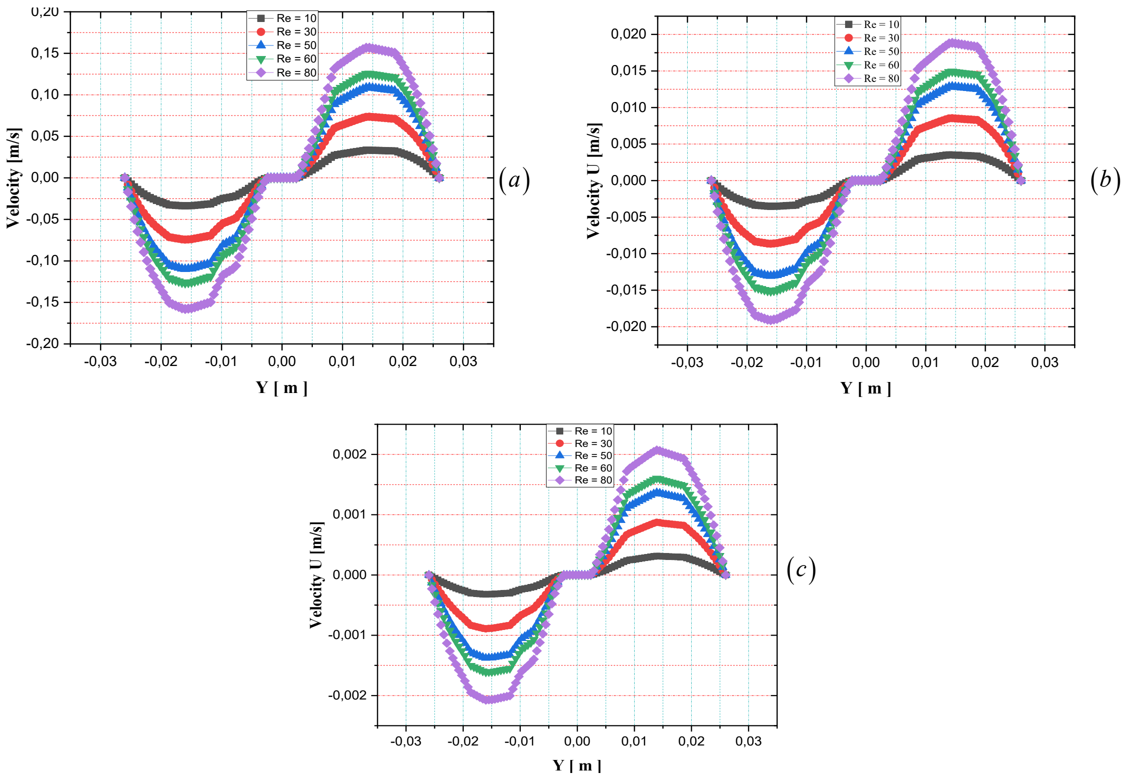

Figure 15: Axial velocity for standard geometries at different Reynolds number values ((a) n = 0.49; (b) n = 0.75; (c) n = 0.93)

The distribution of fluid particle traces in the KMSST, KMSOH, KMSTH, KMSTHH, and KMSFH geometries, particularly at the middle and exit sections of each geometry, is described by the Poincare section (see figure.15-20). The particles of the two fluids that were mixed along the mixers for a specific index of behavior (n = 0.49; 0.75; 0.93), and a generalized Reynolds number of (50; 80), are represented by the red and blue dots.

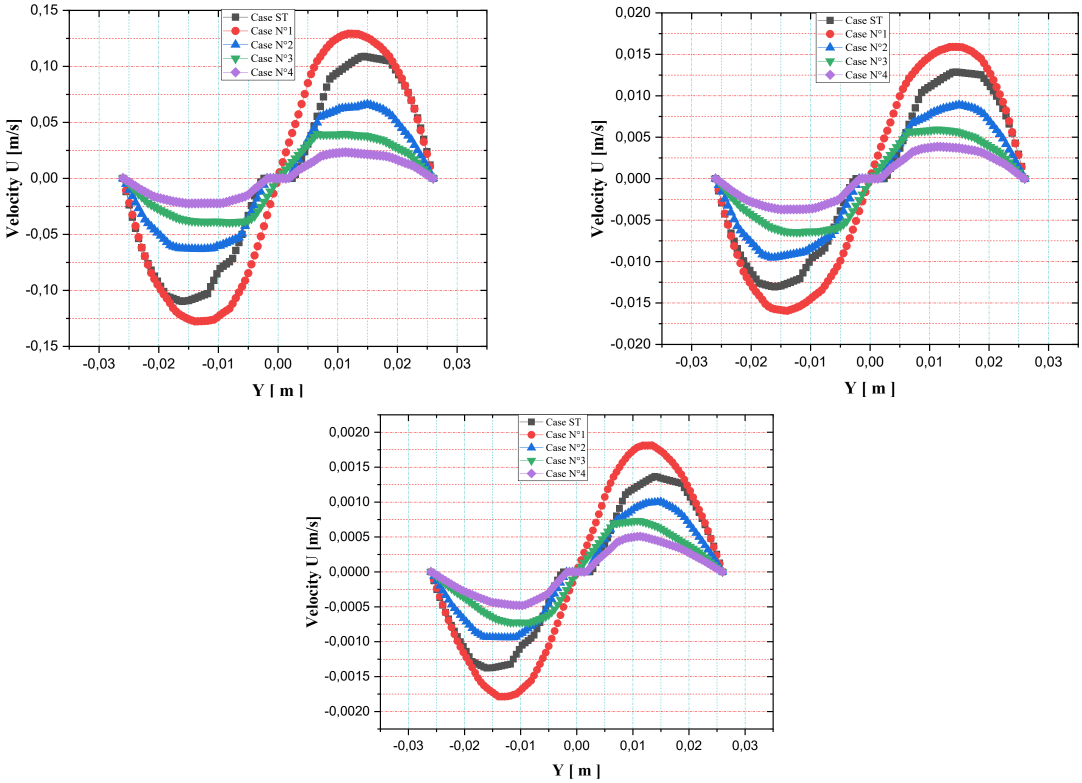

Figure 16: Axial velocity for different geometries for Re= 50, (a) n = 0.49; (b) n = 0.75; (c) n = 0.93)

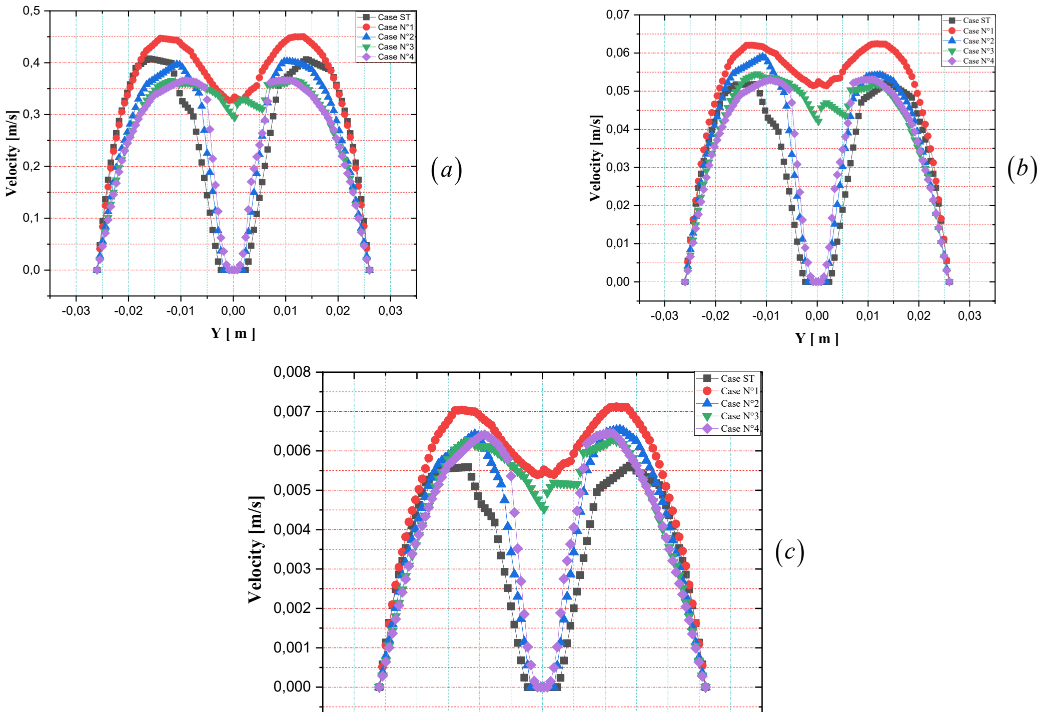

Figure 17: Axial velocity for all geometries for Re= 50, ((a) n = 0.49; (b) n = 0.75; (c) n = 0.93)

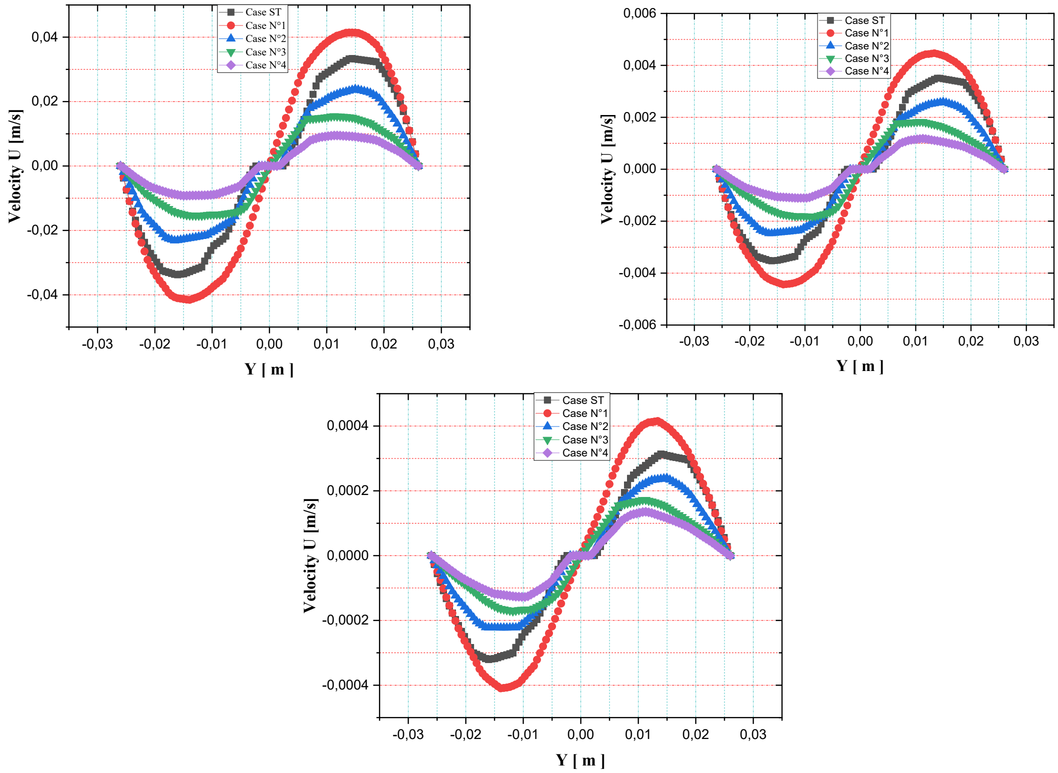

Figure 18: Axial velocity for all geometries for Re = 10, (a) n = 0.49; (b) n = 0.75; (c) n = 0.93)

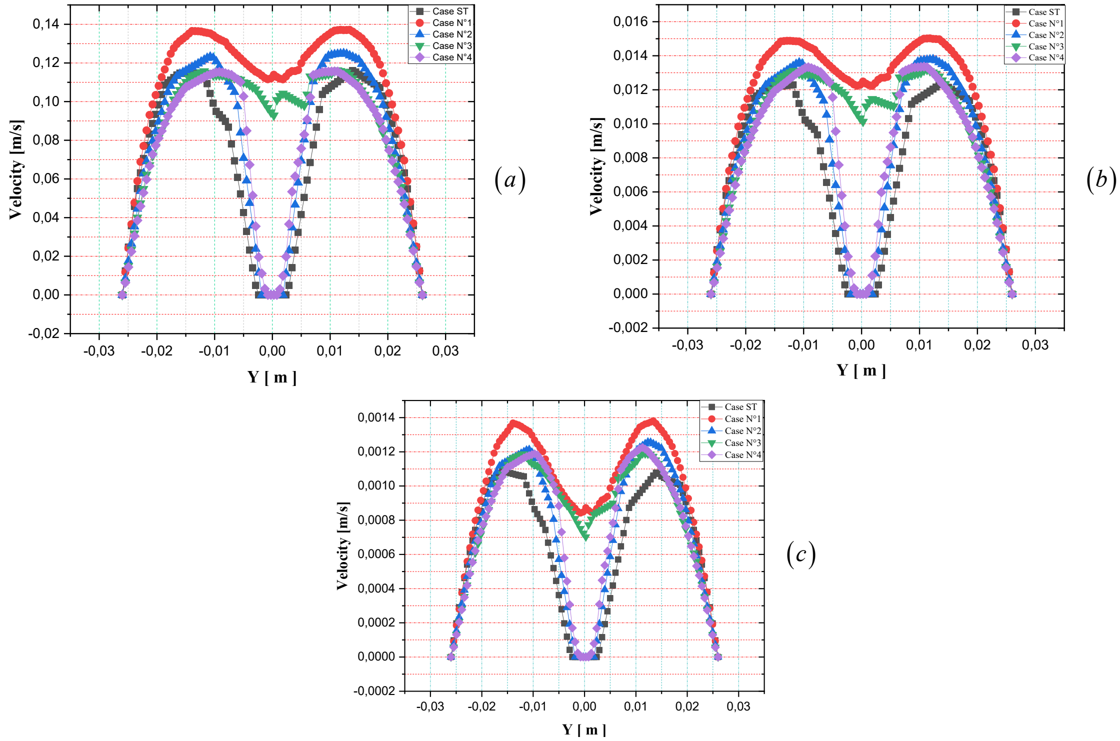

Figure 19: Axial velocity for all geometries for Re= 10, ((a) n = 0.49; (b) n = 0.75; (c) n = 0.93

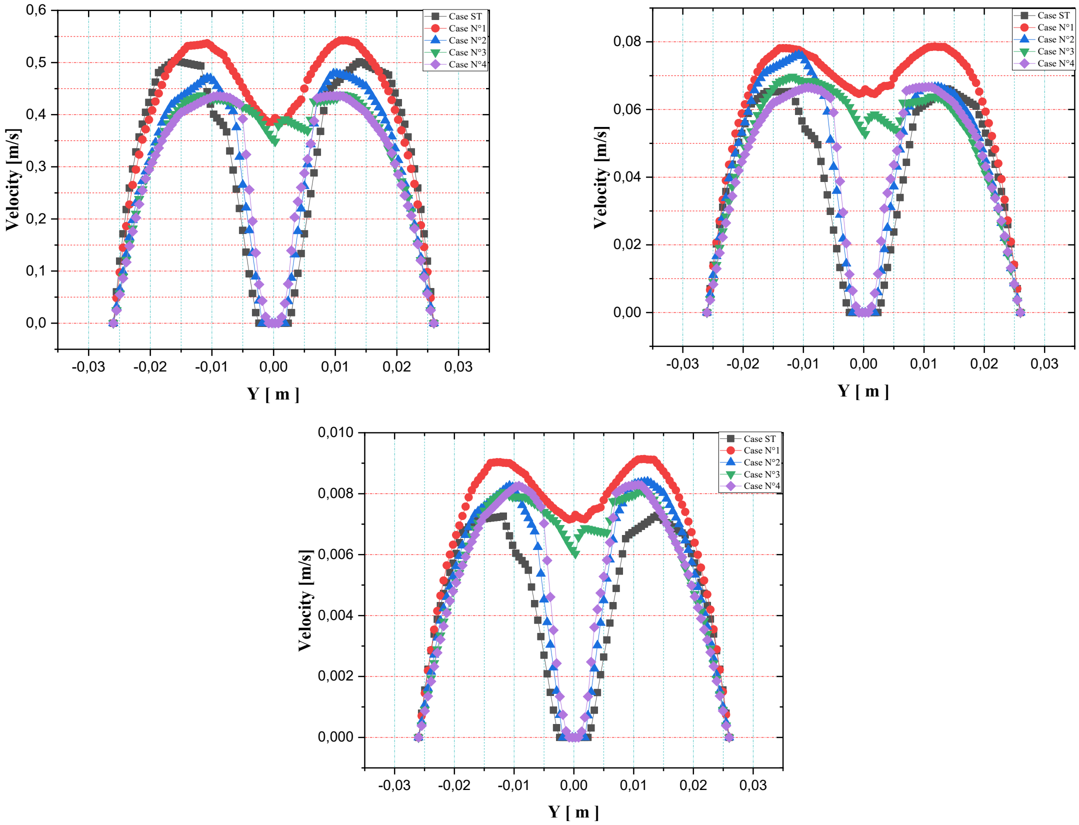

Figure 20: Axial velocity for all geometries for Re= 80, ((a) n = 0.49; (b) n = 0.75; (c) n = 0.93)

9. Pressure drops in the mixer

Pressure drops are the pumping power needed to pump the fluid into the mixer. It is the pressure difference between the inlet and outlet of the channel that was calculated as a difference between the surface weighted averages of the total pressure. In the figure 21 we have compared our supposed geometries.

$$\Delta P = P_{sortie} - P_{ertree} \tag{14}$$

An increase in the mixer mixture's performance is typically accompanied by a pressure drop. For the various values of the behavior index, the pressure differential between the mixer's intake and outlet sections was determined and shown as a function of the Reynolds number, as shown in figure 21. While the pressure drop lowers with an increase in the behavior index (reduction in apparent viscosity), it increases with an increase in the Reynolds number. Its relationship to perceived viscosity is inverse. This causes friction between the fluid layers on one hand and between the fluid and the wall on the other. Above is an illustration of how the perceived viscosity contributed to the rise in friction.

10. Cost of mechanical energy (MEC)

A higher mixing index is associated with higher flows with higher energy consumption. Must be calculated to balance the cost of the mixture with its performance value in terms of input power (Energy required to push the fluid through the channel). The mixing index equation is given by the following formula:

$$MEC = \frac{\Delta P x Q}{MI} \tag{15}$$

Figure 22 clearly shows that the shape of the geometry has a significant effect on the mixing index. This could indicate that the specific geometry of case N°1 favors better mixing of fluids for a given Reynolds number than the other configurations tested.

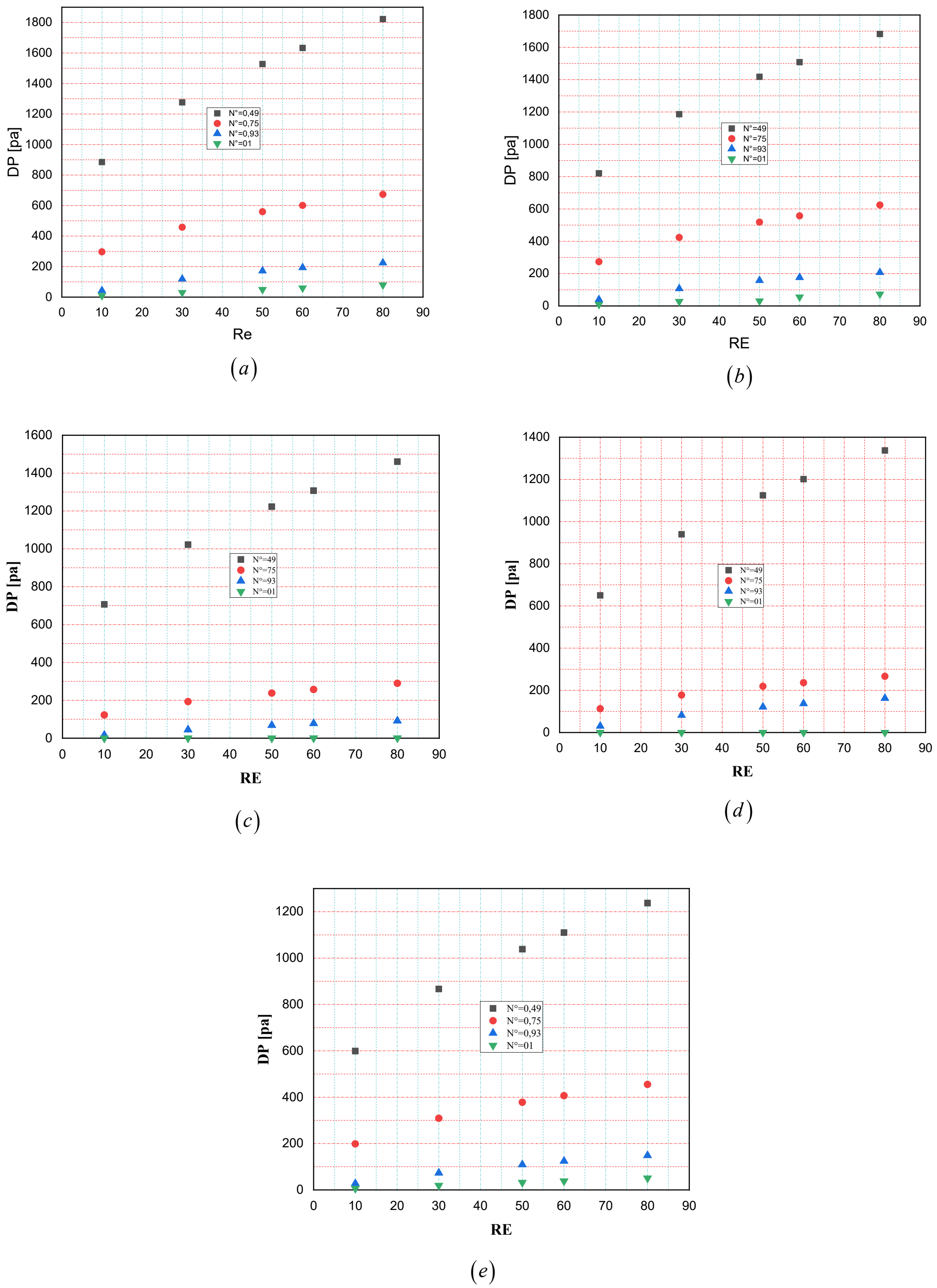

Figure 21: Variation of pressure drops with generalized Reynolds numbers for different behavioral indices (a = KMSST, b = KMSOH, c = KMSTH, d = KMSTHH, e = KMSFH)

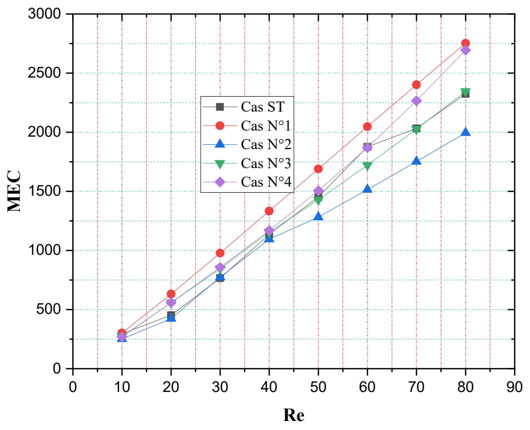

Figure 22: Variation of the energy cost of the mixture as a function of the Reynolds number for the mixers for n = 0.49

11. Conclusion

This study delved into the influence of rheological and geometrical characteristics on the flow structures generated within a KENIC static mixer. The primary objectives centered on examining how these factors impact fluid flow attributes, particularly under low-pressure conditions and concerning mixing efficiency. The investigation encompassed a comprehensive evaluation of different mixer shapes, considering parameters such as mixing index, thermal mixing index, hydrodynamic behavior, and probability density function. The exploration spanned both Newtonian and non-Newtonian fluids, emphasizing Reynolds numbers spanning 10 to 80. Comparative analyses were performed against a conventional static mixer configuration. The comprehensive numerical simulations underscored the pivotal roles played by rheological and geometrical factors in shaping flow behaviors. The findings distinctly highlighted the superior performance of the designated KENIC static mixer configuration, referred to as KMSFH, when contrasted with alternative scenarios. This enhanced performance manifested across diverse flow conditions, showcasing amplified mixing efficiency and reduced pressure losses. Globally, the study revealed that the KMSFH configuration outperformed the other suggested mixers by an impressive margin of 99%.

References

[1] Mahmoodi, H., Razzaghi, K., and Shahraki, F.: Improving mixing performance by curved blade static mixer. AIChE Journal, 66(11), (2020). Doi : 10.1002/aic.17034.

[2] Mashoofi, N., Pourahmad, S., and Pesteei, S. M.: Study the effect of axially perforated twisted tapes on the thermal performance enhancement factor of a double tube heat exchanger. Case studies in thermal engineering, 10, 161-168. (2017). Doi : 10.1016/j.csite.2017.06.001

[3] Al-Fahed, S., Chamra, L. M., and Chakroun, W. : Pressure drop and heat transfer comparison for both microfin tube and twisted-tape inserts in laminar flow. Experimental Thermal and Fluid Science, 18(4), 323-333. (1998). Doi : 10.1016/S0894-1777(98)10037-7

[4] Meng, H., Zhu, G., Yu, Y., Wang, Z., and Wu, J. : The effect of symmetrical perforated holes on the turbulent heat transfer in the static mixer with modified Kenics segments. International Journal of Heat and Mass Transfer, 99, 647-659. (2016). Doi :10.1016/j.ijheatmasstransfer.2016.03.110

[5] Meng, H., Han, M., Yu, Y., Wang, Z., and Wu, J.: Numerical evaluations on the characteristics of turbulent flow and heat transfer in the Lightnin static mixer. International Journal of Heat and Mass Transfer, 156, 119788. (2020). Doi :10.1016/j.ijheatmasstransfer.2020.119788

[6] Meng, H., Meng, T., Yu, Y., Wang, Z., and Wu, J. : Experimental and numerical investigation of turbulent flow and heat transfer characteristics in the Komax static mixer. International Journal of Heat and Mass Transfer, 194, 123006. (2022). Doi : 10.1016/j.ijheatmasstransfer.2022.123006

[7] Abushaikha, A. S., Blunt, M. J., Gosselin, O. R., Pain, C. C., and Jackson, M. D. : Interface control volume finite element method for modelling multi-phase fluid flow in highly heterogeneous and fractured reservoirs. Journal of Computational Physics, 298, 41-61. (2015). Doi : 10.1016/j.jcp.2015.05.024

[8] Mayer-Laigle, C., Gatumel, C., and Berthiaux, H. : Mixing dynamics for easy flowing powders in a lab scale Turbula® mixer. Chemical Engineering Research and Design, 95, 248-261. (2015). Doi : 10.1016/j.cherd.2014.11.003

[9] Belhout, C., Bouzit, M., Menacer, B., Kamla, Y., and Ameur, H.: Numerical study of viscous fluid flows in a kenics static mixer. Mechanics, 26(3), 206-211. (2020). Doi : 10.5755/j01.mech.26.3.24160

[10] Kamla, Y., Ameur, H., Arab, M. I., and Azeddine, B. : Data on the hydrodynamics and power consumption induced by modified anchor impellers in cylindrical tanks. Data in brief, 39, 107669. (2021). Doi : 10.1016/j.dib.2021.107669

[11] Hobbs, D. M., and Muzzio, F. J.: Reynolds number effects on laminar mixing in the Kenics static mixer. Chemical engineering journal, 70(2), 93-104. (1998). Doi: 10.1016/S0923-0467(98)00065-7

[12] Ghanem, A., Lemenand, T., Della Valle, D., and Peerhossaini, H.: Static mixers: Mechanisms, applications, and

characterization methods–A review. Chemical engineering research and design, 92(2), 205-228. (2014). Doi: 10.1016/j.cherd.2013.07.013

[13] Rauline, D., Le Blévec, J. M., Bousquet, J., and Tanguy, P. A.: A comparative assessment of the performance of the Kenics and SMX static mixers. Chemical Engineering Research and Design, 78(3), 389-396. (2000). Doi: 10.1205/026387600527284

[14] Soman, S. S., and Madhuranthakam, C. M. R.: Effects of internal geometry modifications on the dispersive and distributive mixing in static mixers. Chemical Engineering and Processing: Process Intensification, 122, 31-43. (2017). Doi: 10.1016/j.cep.2017.10.001

[15] Ameur, H., Kamla, Y., and Sahel, D.: Performance of helical screw impellers for mixing of viscous liquids in cylindrical reactors. ChemistrySelect, 2(5), 1891-1894. (2017). Doi: 10.1002/slct.201602072

[16] Talhaoui, A., Draoui, B., and Youcefi, A.: Effect of Geometry Design on Mixing Performance of Newtonian Fluids using Helical Overlapped Mixer Elements in Kenics Static Mixer. Journal of Applied Fluid Mechanics, 14(6), 1643-1656. (2021). Doi: 10.47176/JAFM.14.06.32494

[17] Haddadi, M. M., Hosseini, S. H., Rashtchian, D., and Olazar, M.: Comparative analysis of different static mixers performance by CFD technique: An innovative mixer. Chinese Journal of Chemical Engineering, 28(3), 672-684. (2020). Doi: 10.1016/j.cjche.2019.09.004

[18] Ghanem, A., Habchi, C., Lemenand, T., Della Valle, D., and Peerhossaini, H.: Energy efficiency in process industry–High-efficiency vortex (HEV) multifunctional heat exchanger. Renewable Energy, 56, 96-104. (2013). Doi : 10.1016/j.renene.2012.09.024

[19] Ghanem, A., Habchi, C., Lemenand, T., and DELLA, D.: Intensification des transferts convectifs par vorticité longitudinale. In Congrès Français de Thermique. (2011).

[20] Thakur, R. K., Vial, C., Nigam, K. D. P., Nauman, E. B., and Djelveh, G.: Static mixers in the process industries—a review. Chemical engineering research and design, 81(7), 787-826. (2003). Doi : 10.1205/026387603322302968

[21] Fradette, L., Li, H. Z., Choplin, L., and Tanguy, P.: Gas/liquid dispersions with a SMX static mixer in the laminar regime. Chemical engineering science, 61(11), 3506-3518. (2006). Doi :10.1016/j.ces.2005.12.022

[23] Azer, N. Z., Lin, S. T., and Fan, L. T.: Augmentation of forced flow boiling heat transfer with Kenics montionless mixers. Industrial & Engineering Chemistry Process Design and Development, 19(2), 246-250. (1980). Doi :10.1021/i260074a008